ACS APPLIED MATERIALS & INTERFACES

Research Article

www.acsami.org

Novel Phenolic Biosensor Based on a Magnetic Polydopamine-Laccase-Nickel Nanoparticle Loaded Carbon Nanofiber Composite

Dawei Li, Lei Luo, Zengyuan Pang, Lei Ding, Qingqing Wang, Huizhen Ke, Fenglin Huang,* and Qufu Wei*

Key Laboratory of Eco-Textiles, Ministry of Education, Jiangnan University, Wuxi, Jiangsu 214122, China

Supporting Information

ABSTRACT: A novel phenolic biosensor was prepared on the basis of a composite of polydopamine (PDA)-laccase (Lac)-nickel nanoparticle loaded carbon nanofibers (NiCNFs). First, NiCNFs were fabricated by a combination of electrospinning and a high temperature carbonization technique. Subsequently, the magnetic composite was obtained through one-pot Lac-catalyzed oxidation of dopamine (DA) in an aqueous suspension containing Lac, NiCNFs, and DA. Finally, a magnetic glass carbon electrode (MGCE) was employed to separate and immobilize the composite; the modified electrode was then denoted as PDA-Lac-NiCNFs/MGCE. Fourier transform infrared (FT-IR) spectra and cyclic voltammetry (CV) analyses revealed the NiCNFs had good biocompatibility for Lac immobilization and greatly facilitated the direct electron transfer between Lac and electrode surface. The immobilized Lac showed a pair of stable and well-defined redox peaks, and the electrochemical behavior of Lac was a surface-controlled process in pH 5.5 acetate buffer solution. The PDA-Lac-NiCNFs/MGCE for biosensing of catechol exhibited a sensitivity of 25 μA mM^{-1} cm^{-2}, a detection limit of 0.69 μM (S/N = 3), and a linear range from 1 μM to 9.1 mM, as well as good selectivity and stability. Meanwhile, this novel biosensor demonstrated its promising application in detecting catechol in real water samples.

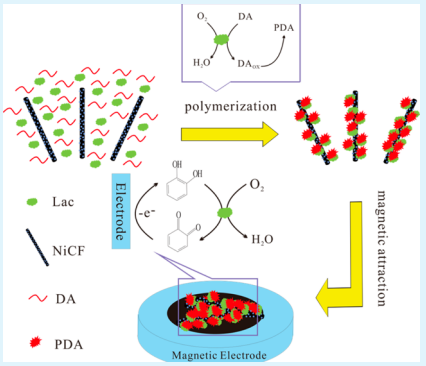

KEYWORDS: *carbon nanofibers, nickel nanoparticle, electrospinning, laccase, dopamine, phenolic biosensor*

INTRODUCTION

Phenol and phenolic compounds, as widespread contaminants, come from both nature and industries.[1] Most phenols are poisonous with different toxicities, and even some chlorophenols and nitrophenols can lead to cancer and loss of immunity in the body.[2] As a consequence, there is an urgent need to exploit simple and high-efficient detection method of phenols. Until now, some available tools for measuring phenols have been employed, such as liquid chromatography, gas chromatography, enzyme immunoassays, electro analytical techniques, etc.[3−5] Although these methods can give precise results at low concentration, their use in online or field monitoring is restricted due to the large size, fixed space location of the analytical apparatuses, and complicated purification process of samples. Compared with those classical testing instruments, the biosensor is simple, fast, facile, and amenable to miniaturization in analytical equipment which meets the requirements for application to multicomponent solutions in situ.[1]

Laccase (Lac) is a multicopper oxidase, which can catalyze the oxidation of phenolic substrates with the accompanying reduction of molecular oxygen to water.[6] On the basis of this, a variety of biosensors using Lac have been developed for the detection of phenolic compounds.[2,7−10] Recently, a tremendous amount of research work has focused on developing reagentless enzyme electrodes, which can realize direct electron transfer (DET) by combining enzymes with conductive materials.[8,11−14] Carbon materials, such as carbon nanotube,[9] carbon black,[15] mesoporous carbon,[16] graphene,[2] and carbon nanofiber (CNF),[17] have been widely employed as the immobilization materials of enzymes in biosensors, which can be attributed to their large specific surface area, excellent conductivity, and satisfactory biocompatibility. Among these materials, CNF possesses much larger functionalized surface area compared to that of CNT and is more suitable for immobilization and stability of enzyme. It has been proven that CNF is an outstanding matrix for the development of biosensors, which is far superior to the carbon nanotube.[17]

Notably, the CNF possesses a history of more than a century; the carbon filaments discovered in 1889 may be the earliest CNF.[18] After more than a century of development, various methods used for CNF preparation have been developed, such as arc-discharge,[19] laser ablation,[20] chemical vapor deposition (CVD) methods,[21] and others. Electrospinning, known as a facile and convenient process technique, produces nanofibers or microfibers with different diameters using a variety of polymers. Carbonization of electrospun polyacrylonitrile nanofibers can be employed to fabricate CNF.[22] In addition, to our best knowledge, CNF from CVD usually contains some impurities, e.g., metal catalyst and graphite particle, which requires a further complicated

Received: January 18, 2014
Accepted: March 7, 2014
Published: March 7, 2014

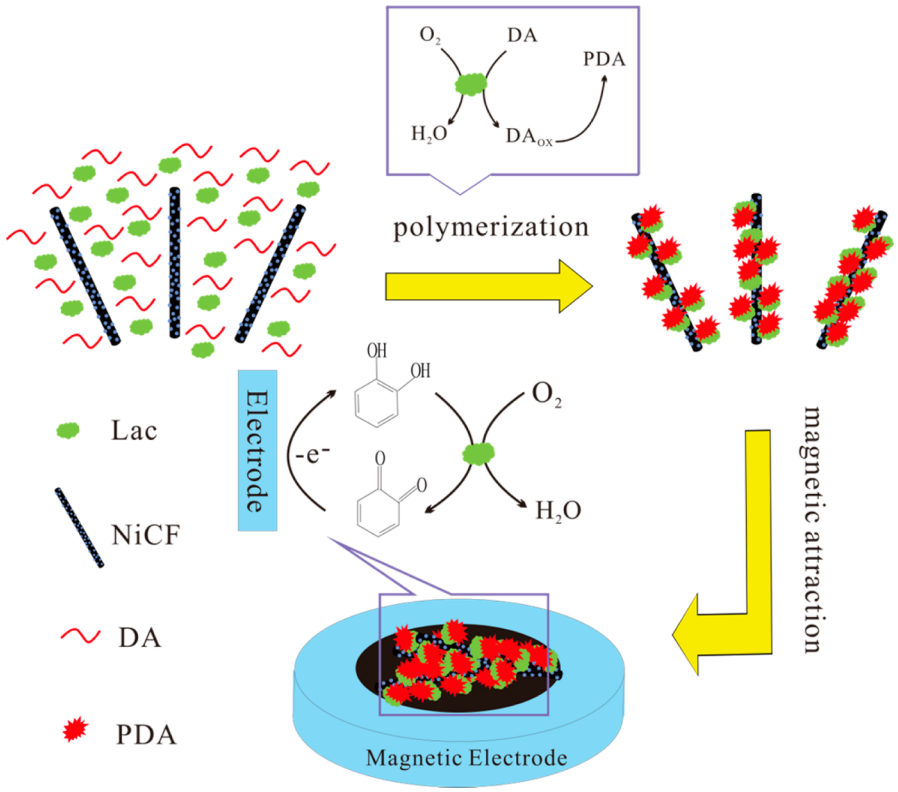

Figure 1. Schematic preparation of PDA-Lac-NiCNFs composite and biosensors.

purification process, while the electrospun CNF (ECNF) exhibits a simple fabrication process and higher purity. Nowadays, some nonenzymatic electrochemical sensors based on ECNF or catalytic metal nanoparticle/ECNF composite have been reported.[23−26] ECNF showed a great potential for biosensing applications.

Magnetic nanoparticles have been widely applied in biocatalysis,[27] separation/purification of proteins,[28] drug delivery, medical imaging,[29] and biosensors.[7] The introduction of magnetic nanoparticles in the biosensor not only improves sensitivity but also offers a controllable immobilization method of biomolecules. Interestingly, an external magnetic field can control electrocatalytic and bioelectrocatalytic processes of functionalized magnetic particles associated with electrodes.[30] Some facile biosensors based on magnetic electrodes have been reported.[7,31,32] Dopamine (DA) is a pivotal neurotransmitter of redox activity, existing in the brains and bodies of animals, which has attracted wide attention from biosensor scientists,[33−35] and the self-polymerization of DA, which generates polydopamine (PDA) with good biocompatibility, has been applied in biosensing and multifunctional coating.[7,36]

In this paper, we developed a novel Lac-based biosensor utilizing electrospun nickel nanoparticle loaded carbon nanofibers (NiCNFs) for the first time. The PDA-Lac-NiCNFs composite was synthesized through one-pot Lac-catalyzed oxidation of dopamine (DA) in an aqueous suspension containing Lac, NiCNFs, and DA. After that, a PDA-Lac-NiCNFs/magnetic glass carbon electrode (MGCE) was prepared by simple and efficient magnetic separation/immobilization of the PDA-Lac-NiCNFs composite. Finally, the PDA-Lac-NiCNFs/MGCE was employed to detect a hazardous phenolic compound, catechol, in a water environment, which exhibited better performance than those Lac-based biosensors reported earlier. This study demonstrates that the electrospun nickel nanoparticle loaded carbon nanofiber is a competitive material in the field of biosensing and offers strong theoretical and technical support for designing a high-efficient phenolic biosensor serving as an environmental monitor.

EXPERIMENTAL PROCEDURES

Reagents and Materials. PAN (average molecular weight = 79,100) powder and laccase (from Trametes, activity ≥10 U/mg) were obtained from Sigma-Aldrich and used without further purification. *N*,*N*-Dimethylformamide (DMF) with a purity of 99.5% was used as received. Nickel acetate tetrahydrate ($C_4H_6NiO_4{\cdot}4H_2O$) was purchased from the Sinopharm Group Chemical Reagent Co., Ltd. (Shanghai, China). Dopamine and catechol were purchased from Aladdin Chemical Reagent Co., Ltd. (Shanghai, China). There are no special instructions; acetate buffer solution (0.2 M HAc-NaAc, pH = 5.5) was used as a supporting electrolyte. All aqueous solutions were prepared with deionized water (DIW).

Apparatus. Fourier transform infrared (FT-IR) spectra were recorded in the range of 500−4000 cm^{-1} on a Nicolet iS10 FT-IR spectrometer (Thermo Fisher Scientific). KBr pellet was used to prepare the samples for FT-IR measurements. The morphologies of NiCNFs and PDA-Lac-NiCNFs composite were observed with a Hitachi SU1510 SEM and a high-resolution transmission electron microscope (TEM, JEOL/JEM-2100, Japan). Prior to scanning under the SEM, the NiCNFs and PDA-Lac-NiCNFs composite were sputter coated for 90 s with gold to avoid charge accumulations. Energy dispersive X-ray spectroscopy (EDX) and powder D8 Advance X-ray diffraction (XRD, Bruker AXS D8) were employed to analyze the chemical components of the NiCNFs. Electrochemical experiments were carried out at room temperature using a CHI 660D electrochemical workstation (CH Instruments, Inc., Austin, USA). A three-electrode cell with a magnetic glass carbon electrode (MGCE) (3.0 mm in diameter, purchased from Gaoss Union Technology Co., Ltd., Wuhan, China), a platinum wire auxiliary electrode, and an Ag/AgCl reference electrode were used for electrochemical measurements.

dx.doi.org/10.1021/am500375n | ACS Appl. Mater. Interfaces 2014, 6, 5144−5151

The electrolyte solution was bubbled with highly pure nitrogen for 15 min before the electrochemical experiments, and a nitrogen atmosphere was kept for the solution throughout the experiments except the amperometric experiments for the laccase biosensor.

Synthesis of NiCNFs. The NiCNFs were prepared by the following steps. First, the electrospinning solution was prepared by dissolving 12 wt % PAN powders and 5 wt % $C_4H_6NiO_4{\cdot}4H_2O$ with magnetic stirring for 8 h. Second, the prepared solution was added into a syringe for electrospinning. The experimental parameters were set with a voltage of 15 kV, a working distance of 15 cm, and a flow rate of 1 mL/h, respectively. Finally, a high temperature furnace was employed to stabilize and carbonize the PAN nanofibers. The whole process was conducted in N_2 atmosphere and could be divided into two phases: (1) heating up to 280 °C with a rate of 2 °C min^{-1} and keeping this temperature for 1 h (this process was for stabilizing the shape of the nanofibers); (2) heating up to 900 °C with a rate of 5 °C min^{-1} to carbonize the nanofibers, maintaining at the highest temperature for 2 h, and then cooling down to room temperature.

Preparation of PDA-Lac-NiCNFs Composite and Biosensors. The NiCNFs were ground to short fibers using a mortar before use. The PDA-Lac-NiCNFs composite was prepared as shown in Figure 1. The mixture of 1.0 mg mL^{-1} Lac and 1.5 mg mL^{-1} NiCNFs (final concentration for each) was added into 1.0 mL of 0.2 M acetate buffer solution (pH 5.5) containing 15 mM DA under stirring. It took almost 3 h for the complete polymerization of DA. The reaction product (PDA) could wrap the Lac on the surface of the NiCNFs, from which the PDA-Lac-NiCNFs composite was obtained.

Prior to modification, the MGCE was successively polished to a mirror-like surface with 1.0, 0.3, and 0.05 μm alumina slurry and then rinsed thoroughly by DIW. Afterward, the electrode was washed with anhydrous ethanol for 3 min in an ultrasonic bath to remove the loosely adsorbed alumina slurry. Finally, the treated electrode was dried with a stream of nitrogen. As shown in Figure 1, 10 μL of PDA-Lac-NiCNFs aqueous suspension was cast onto the bare MGCE. The PDA-Lac-NiCNFs composite was attracted toward the surface of electrode immediately, and the modified electrode was washed by DIW for three times, dried at room temperature, and stored at 4 °C in a refrigerator before use. For comparison, PDA-Lac/MGCE and NiCNFs/MGCE were fabricated in a similar way, ensuring the equal amounts of DA, Lac, and NiCNFs.

RESULTS AND DISCUSSION

Characterizations. Figure 2 shows the FT-IR spectra of pure DA (a), pristine Lac (b), PDA-Lac composite (c), and PDA-Lac-NiCNFs composite (d). As shown in Figure 2a, the absorption peaks at 1500 and 1288 cm^{-1} are assigned to benzene ring C−C vibration of DA and the C−O stretching of phenolic OH, respectively.[37] It can be seen from Figure 2b that a broad peak centered at 3350 cm^{-1} can be attributed to NH and OH stretching vibrations in the protein,[38] and the peaks at 1670 and 1580 cm^{-1} are related to the characteristic absorption peaks of amide I (1700−1600 cm^{-1}) and amide II (1600−1500 cm^{-1}) in native laccase.[39] Figure 2c,d displays similar absorption peaks; however, the peaks related to DA and Lac showed a decrease in intensity. The peak at 1670 cm^{-1} disappeared completely, which may be caused by the interaction between Lac and DA. The FT-IR analyses proved that PDA-Lac composite was successfully prepared and the addition of NiCNFs did not affect the chemical groups of the composite, which also demonstrated the satisfactory biocompatibility of NiCNFs. The Lac-catalyzed synthesis of PDA-Lac-NiCNFs composite was verified in Figure S1, Supporting Information. As shown in Figure S1a, Supporting Information, after three hours of polymerization reaction, the composite with good hydrophilicity dispersed evenly in the solution. However, after applying a magnetic field by a magnet (see Figure S1b, Supporting Information), the PDA-Lac-NiCNFs composite aggregated promptly and the color of the solution became much more transparent, indicating that most of the PDA-Lac-NiCNFs composite possessed magnetic action.

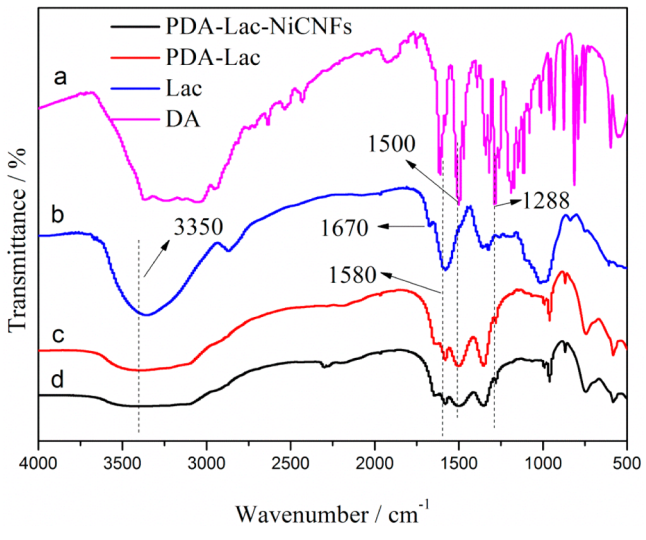

Figure 2. FT-IR spectra of pure DA (a), pristine Lac (b), PDA-Lac composite (c), and PDA-Lac-NiCNFs composite (d).

Figure 3a shows the surface morphology of PDA-Lac-NiCNFs/MGCE. It can be clearly seen that the short NiCNFs dispersed well in the PDA-Lac-NiCNFs composite. Most of them were embedded into the composite, which would play a role of "molecular wires" connecting the active center of Lac and the surface of MGCE. Actually, the composite formed a membrane on the surface of electrode. Besides, there were some "pores" or "ravines" existing in the membrane, which were beneficial to the diffusion of substrate. The morphology of NiCNFs is shown in Figure 3b. The randomly distributed NiCNFs formed a fibrous web, and many NiCNFs were broken up into short fibers because the thermal treatment process enabled the fibers to become fragile. It is noticeable that some particles can be observed on the surface of NiCNFs. The TEM image of NiCNFs (see Figure S2a, Supporting Information) illustrates that the nanoparticles were embedded in the carbon nanofibers matrix. The EDX result (see Figure S2b, Supporting Information) indicates that the main elements of NiCNFs are C and Ni. The Kα line of O is attributed to the oxygen in air, and the Kα and Kb lines of Cu are caused by the used copper mesh in the process of sample preparation. XRD characterization was applied to further investigate the composition of NiCNFs, and the result is illustrated in Figure S3, Supporting Information. It shows four characteristic diffraction peaks at

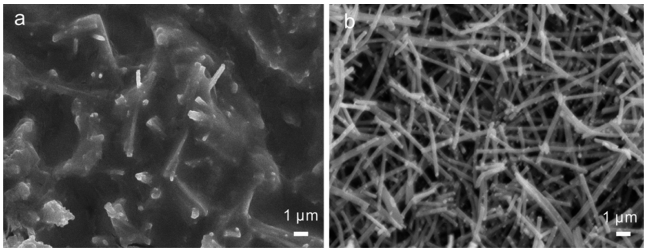

Figure 3. SEM images of the surface of PDA-Lac-NiCNFs/MGCE (a) and NiCNFs (b).

25.6°, 44.5°, 51.8°, and 76.4°, which corresponded to the (002) plane of carbon and (111), (200), and (220) crystalline planes of fcc Ni, respectively. The XRD result provides evidence confirming the existence of Ni nanoparticles in the composite.

Cyclic voltammetry (CV) was used to characterize the modified electrodes in 0.1 M KCl and 1 mM $Fe(CN)_6^{3-/4-}$ solution. Figure 4 compares the CVs response at bare MGCE,

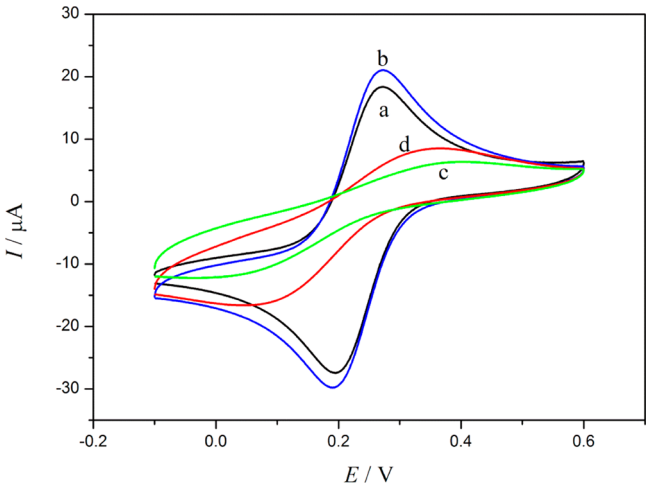

Figure 4. Cyclic voltammograms of bare MGCE (a), NiCNFs/MGCE (b), PDA-Lac/MGCE (c), and PDA-Lac-NiCNFs/MGCE (d) in 0.1 M KCl and 1 mM $Fe(CN)_6^{3-/4-}$ solution at a scan rate of 100 mV s^{-1}.

NiCNFs/MGCE, PDA-Lac/MGCE, and PDA-Lac-NiCNFs/MGCE in the above solution. Compared with bare MGCE, all the redox peaks of NiCNFs/MGCE increased, indicating the NiCNFs improved the surface area of electrode substantially. Notably, the anodic and cathodic peak currents on the PDA-Lac/MGCE and PDA-Lac-NiCNFs/MGCE all showed a significant decrease. It may be attributed that the PDA and Lac were nonconductive and hindered the electron transfer. However, the response current on PDA-Lac-NiCNFs/MGCE was higher than that on PDA-Lac/MGCE, which indicated that the NiCNFs improved the conductivity of the composite membrane.

DET of Lac on the PDA-Lac-NiCNFs/MGCE. Figure 5 depicts typical cyclic voltammograms of different electrodes in pH 5.5 acetate buffer solution at a scan rate of 100 mV s^{-1}. No redox peaks were observed for the bare MGCE (a) and NiCNFs/MGCE (b), which demonstrated the electrochemical inertness of NiCNFs within the potential window. The voltammogram of PDA-Lac/MGCE (c) shows poorly defined peaks while that of PDA-Lac-NiCNFs/MGCE (d) shows a pair of well-defined and stable redox peaks, which can be attributed to the DET between the electroactive center of the immobilized Lac and the electrode surface. Herein, the NiCNFs play an important role as "molecular wires" which can build an efficient electron-conducting tunnel. Meanwhile, it can be easily seen that the anodic (Epa) and cathodic (Epc) peak potentials are located at 0.222 and 0.091 V (vs Ag/AgCl), respectively. The formal potential ($E^{0\prime}$) is ca. 0.16 V, and the peak-to-peak separation (ΔE_p) is 131 mV at the scan rate of 100 mV s^{-1}, indicating a fast electron transfer.

As shown in Figure S4a, Supporting Information, with the increase of the scan rate, the Epa shifted to a more positive value and the Epc shifted to a more negative value. Notably, the anodic and cathodic peak currents increased linearly with the

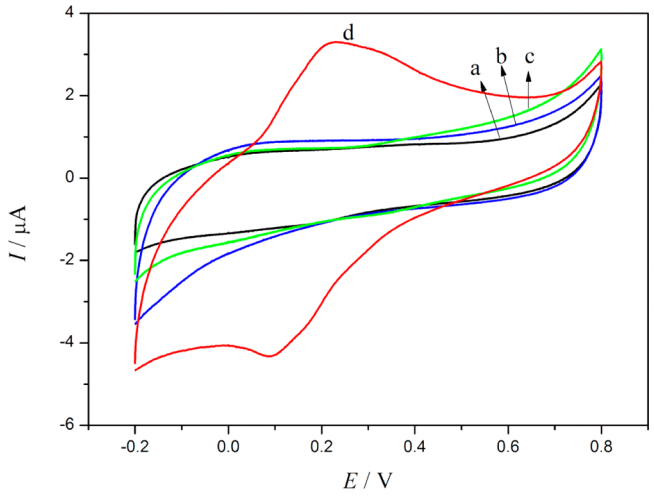

Figure 5. Cyclic voltammograms of bare MGCE (a), NiCNFs/MGCE (b), PDA-Lac/MGCE (c), and PDA-Lac-NiCNFs/MGCE (d) in 0.2 M acetate buffer solution (pH 5.5) at a scan rate of 100 mV s^{-1}.

scan rate from 50 to 400 mV s^{-1} (Figure S4b, Supporting Information), which proved that the electrochemical process is a surface-controlled electrode process. The above experiments demonstrated that the composite can provide a biocompatible environment for the immobilization of Lac, and the NiCNFs facilitated the DET of Lac to a large extent. The charge-transfer coefficient and the apparent electron-transfer rate constant (k_s) of the Lac at the PDA-Lac-NiCNFs/MGCE are estimated to be 0.5 and 1.79 s^{-1} at a scan rate of 100 mV s^{-1} based on the Laviron equation.[40] This value is much larger than that of 0.5 s^{-1} reported for the DET between laccase and the surface of an AuNP-modified GCE,[10] that of 1.17 s^{-1} reported for the laccase immobilized on a AP-rGO/Chit/GCE,[41] and the value of 1.28 s^{-1} observed for the laccase immobilized on Au nanoparticles encapsulated-dendrimer bonded conducting polymer.[42] This might be attributed to the excellent biocompatibility of PDA-NiCNFs composite and the high electron conductivity of NiCNFs. The surface coverage of electroactive species (Γ, in mol cm^{-2}) on electrode could be calculated by applying the formula $Q = nFA\Gamma$, where Q is the charge consumed (C), A is the electrode area (cm^2), F is the Faraday constant, and n is the number of electrons transferred. The calculated surface coverage for the electroactive laccase is 8.31×10^{-10} mol cm^{-2}, which is higher than the theoretically calculated value reported in a previous study (1.3×10^{-11} mol cm^{-2}).[39] This result indicates that more Lac was immobilized in the PDA-NiCNFs composite due to the large specific surface area of NiCNFs.

The effect of pH on the CVs of the PDA-Lac-NiCNFs/MGCE in 0.2 M acetate buffer solution was also investigated. As can be seen in Figure S5a, Supporting Information, the redox peaks moved left gradually as pH value changed from 3.0 to 7.0. The values of the Epa, Epc, and $E^{0\prime}$ shifted negatively and linearly with an increased solution pH (see Figure S5b, Supporting Information), indicating that proton transfer occurred in the electrochemical process. The Plots of Epa, Epc, and $E^{0\prime}$ vs pH have a linear relationship with the slopes of −46.8 mV pH^{-1} (r^2 = 0.9936), −52.7 mV pH^{-1} (r^2 = 0.9913), and −49.7 mV pH^{-1} (r^2 = 0.9986), respectively. These values are close to the expected value of −59.2 mV pH^{-1} (25 °C), which indicates that one proton (H^+) and one electron (e^-)

dx.doi.org/10.1021/am500375n | ACS Appl. Mater. Interfaces 2014, 6, 5144−5151

participated in the direct electrochemical reaction of Lac immobilized on the PDA-Lac-NiCNFs/MGCE.[10]

Electrocatalysis of the Electrodes. Figure 6 shows the CVs of different electrodes in 0.2 M acetate buffer solution (pH

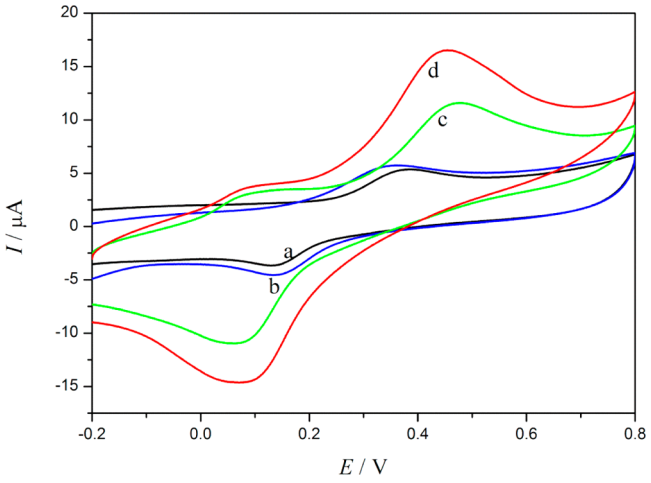

Figure 6. Cyclic voltammograms of bare MGCE (a), NiCNFs/MGCE (b), PDA-Lac/MGCE (c), and PDA-Lac-NiCNFs/MGCE (d) in 0.2 M acetate buffer solution (pH 5.5) containing 1 mM catechol at a scan rate of 100 mV s^{-1}.

5.5) containing 20 μM catechol. A pair of redox peaks can be observed on the bare MGCE, which can be attributed to the redox reaction of catechol. Compared with the bare MGCE, the NiCNFs/MGCE exhibited higher redox peak currents and smaller peak-to-peak separation due to the enhanced electrode surface area and excellent conductivity of NiCNFs, while the PDA-Lac/MGCE and PDA-Lac-NiCNFs/MGCE displayed much higher redox peaks currents, which were attributed to high-efficient catalysis of Lac toward catechol. The reaction mechanism is illustrated in Figure 7. First, the catechol on contact with the Lac was oxidized to 1,2-benzoquinone in the presence of molecular oxygen. Subsequently, the 1,2-benzoquinone was reduced electrochemically on the surface of the MGCE. The obtained current in the process of electrochemical reduction of the 1,2-benzoquinone to catechol was proportional to the concentration of catechol. Besides, the current values on PDA-Lac-NiCNFs/MGCE were larger than those on PDA-Lac/MGCE, indicating the addition of NiCNFs improved the electrocatalysis of the composite toward catechol, which could be attributed to the DET caused by NiCNFs and the concerted electrocatalysis of nickel nanoparticles.

Condition Optimization of the PDA-Lac-NiCNFs/MGCE. To acquire the optimal amperometric response, we investigated the effects of the solution pH and applied potential on the current values respectively. As shown in Figure 8a, the current value reaches the peak at pH 5.5 and then shows a dramatic decrease. Figure 8b presents the influence of different applied potentials on the amperometric responses. It can be clearly seen that the maximum current value comes at 0.4 V; so, 0.2 M acetate buffer solution with pH 5.5 was used, and the applied potential was set at 0.4 V in the following experiments.

Amperometric Biosensing of Catechol. The steady-state amperometric responses of the PDA-Lac-NiCNFs/MGCE and PDA-Lac/MGCE to different concentrations of catechol were determined by the successive addition of different volumes of 2 and 200 mM catechol into 20 mL of pH 5.5 acetate buffer solution with stirring under the optimum conditions. It can be seen from Figure 9a that, with the successive addition of catechol, the steady-state current values gradually increased. The inset in Figure 9a displays the magnified image before 500 s. The first current step for the PDA-Lac-NiCNFs/MGCE happened when adding 20 nM catechol into the acetate buffer solution. Obviously, compared with the PDA-Lac/MGCE, the PDA-Lac-NiCNFs/MGCE showed higher response sensitivity toward catechol. The calibration curves are shown in Figure 9b; the PDA-Lac-NiCNFs/MGCE and the PDA-Lac/MGCE showed a linear range (LR) of 1 μM to 9.1 mM with linearity regression equation (LRE) of $\Delta i(\mu A) = 0.692 + 0.018c$ (μM) ($r^2 = 0.991$), a sensitivity of 18 μA mM^{-1} cm^{-2}, and a limit of detection (LOD) of 0.69 μM (S/N = 3) and a LR of 5 μM to 4.2 mM with LRE of $\Delta i(\mu A) = 0.342 + 0.008c$ (μM) ($r^2 = 0.993$), a sensitivity of 8.3 μA mM^{-1} cm^{-2}, and a LOD of 2.8 μM (S/N = 3), respectively. Table 1 compares biosensing performance of several laccase modified electrodes toward catechol. Our biosensor shows low detection limit, the widest linear range, and reasonable sensitivity. Such wide linear range can be attributed to the fact that the NiCNFs with big surface area offered more active sites for the immobilization of Lac and the nickel nanoparticles played a role of concerted catalysis during the reaction process. According to the Michaelis–Menten equation, $\Delta i = \Delta i_{max} c/(K_M^{app} + c)$ (here, Δi is the steady-state current response of substrate, Δi_{max} is the maximum current response under the condition of saturated substrate, c is the concentration of substrate, and K_M^{app} is the apparent Michaelis–Menten constant); the values of K_M^{app} for

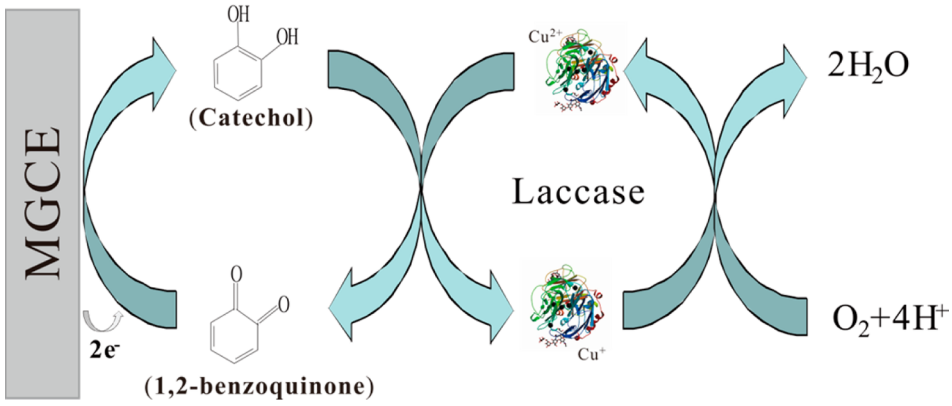

Figure 7. Schematic representation of laccase catalyzed oxidation of catechol with its subsequent electrochemical reduction on the MGCE.

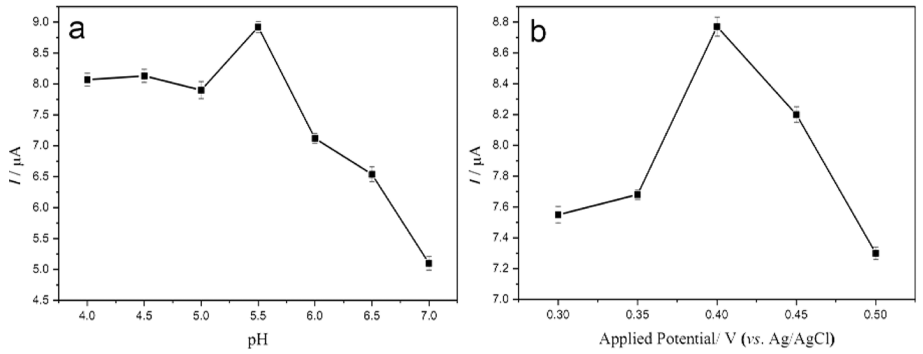

Figure 8. Effect of solution pH (a) and applied potential (b) on the steady-state current response of PDA-Lac-NiCNFs/MGCE in 0.2 M acetate buffer solution containing 500 μM catechol.

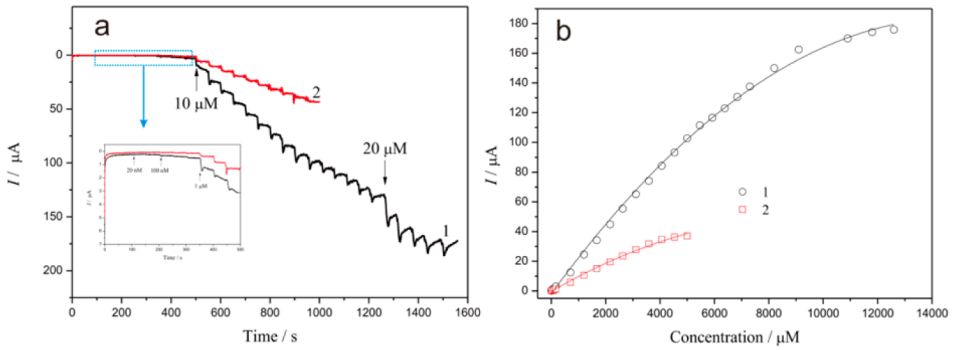

Figure 9. (a) Chronoamperometric responses of (1) PDA-Lac-NiCNFs/MGCE and (2) PDA-Lac/MGCE on successive addition of different concentration and volume of catechol solutions into pH 5.5, 0.2 M acetate buffer solution; applied potential: 0.4 V. Inset: A magnification of the lines before 500 s. (b) The calibration curves with nonlinear fitting.

Table 1. Biosensing Performance Comparison of Different Laccase Modified Electrodes toward Catechol[a]

electrode description	detection limit (μM)	linear range (μM)	sensitivity (μA mM^{-1} cm^{-2})	reference
laccase/CNTs−CS/GCE	0.66	1.2—30	–	43
Lac/AP-rGOs/Chit/GCE	7	15—700	15.79	2
MB-MCM-41/PVA/lac	0.331	4—87.98	–	44
Cu-OMC/Lac/CS/Au	0.67	0.67—13.8	104	45
Lac-FSM7.0-GC	2	2—100	–	8
Lac−GAfCS−MWCNTs/GC	0.02	0.1—50	–	9
PDA-Lac-NiCNFs/MGCE	0.69	1—9100	25	this work

[a]The dashes in the table represent values that were not reported in the references.

PDA-Lac-NiCNFs/MGCE and PDA-Lac/MGCE were calculated to be 7.8 and 3.1 mM, respectively. A smaller K_M^{app} means that Lac immobilized on PDA-Lac/MGCE possessed higher enzymatic activity and showed higher affinity for substrate.

Stability and Reproducibility of the PDA-Lac-NiCNFs/MGCE. The PDA-Lac-NiCNFs/MGCE showed good repeatability, reproducibility, and stability. The relative standard deviation (RSD) of the biosensor response to catechol was within 2.0% for 10 successive measurements, indicating the biosensor has good repeatability. Five biosensors were prepared under the same conditions independently to study the electrode-to-electrode reproducibility and the RSD of the five modified electrodes was 3.1%, indicating the biosensor possess good reproducibility. After a week of storage in 0.2 M, pH 5.5 acetate buffer solution at 4 °C, the current response of the biosensor was almost stable. Even after 30 days, the current response retained 91.7% of the initial value, indicating that the Lac well preserved its activity in the composite of PDA-Lac-NiCNFs, and therefore, the biosensor exhibited good stability.

Selectivity Study and Real Sample Analysis. Catechol and some other phenolic compounds, including catechin, epicatechin, gallic acid, guaiacol, phenol, and aminophenol, were used to determine the selectivity of the biosensor (Figure 10). Obviously, the highest response was 100% for catechol. However, the biosensor almost exhibited no response to other phenolic compounds. Hence, the biosensor showed excellent selectivity for catechol.

To demonstrate the practical application of the biosensor, we investigated the response of the sensor in real water samples. First, all water samples including tap water from our lab and Taihu Lake water from Taihu Lake were filtered with a 0.22 μM membrane and then added to 0.2 M acetate buffer solution (pH 5.5) (2-fold dilution). After that, a diluted sample solution was added into 20 mL of stirred 0.2 M air-saturated acetate buffer solution (pH 5.5). When the current became stable, 100 μM catechol was added into the stirred solution for amperometric detection by the PDA-Lac-NiCNFs/MGCE at 0.4 V, and the experiment was repeated five times. The results are illustrated

dx.doi.org/10.1021/am500375n | ACS Appl. Mater. Interfaces 2014, 6, 5144−5151

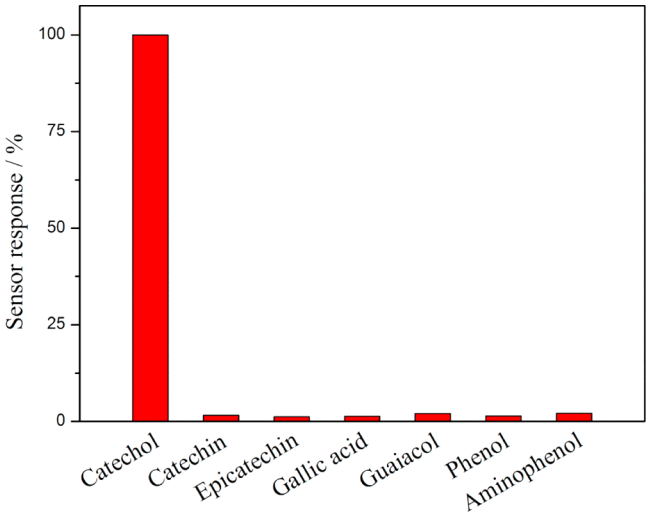

Figure 10. Relative responses of the biosensor for different phenolic compounds (catechol, catechin, epicatechin, gallic acid, guaiacol, phenol, and aminophenol; 100 μM in pH 5.5 acetate buffer solution, respectively).

in Table 2. The recoveries look satisfactory, confirming the potential application of the biosensor in detecting phenols in real samples.

Table 2. Determination of Catechol in Real Water Samples (n = 5)

sample[b]	C_{added} (μM)	C_{found} (μM)	recovery (%)	RSD (%)
1	100	99.1	99.1	1.7
		102.1	102.1	
		98.7	98.7	
		98.1	98.1	
		101.3	101.3	
2	100	102.2	102.2	2.9
		97.2	97.2	
		103.2	103.2	
		97.9	97.9	
		97.3	97.3	

[b]1: tap water, 2: Taihu Lake water.

CONCLUSIONS

In summary, a PDA-Lac-NiCNFs composite was synthesized through a one-pot Lac-catalyzed oxidation of DA in an aqueous suspension containing Lac, NiCNFs, and DA. A novel phenolic biosensor was successfully prepared by facile and efficient magnetic separation/immobilization of the PDA-Lac-NiCNFs composite on a magnetic glass carbon electrode. Herein, the NiCNFs, as a type of one-dimensional magnetic material, possess large specific surface area and numerous nickel nanoparticles, offering abundant active sites for the immobilization of Lac, and the novel biosensor displayed outstanding electrocatalysis toward catechol with wide linear range and low detection limit. Furthermore, the biosensor also showed good repeatability, reproducibility, and stability, attributed to the excellent biocompatible microenvironment of the composite matrix. Finally, the biosensor was successfully applied in detecting catechol in real samples. This study demonstrates that the PDA-Lac-NiCNFs composite is a good candidate for the construction of a highly sensitive phenolic biosensor.

ASSOCIATED CONTENT

Supporting Information

Additional figures as depicted in the Article. This material is available free of charge via the Internet at http://pubs.acs.org.

AUTHOR INFORMATION

Corresponding Authors

*E-mail: qfwei@jiangnan.edu.cn. Tel: (+86)510-85912007. Fax: (+86)510-85913100.

*E-mail: flhuang@jiangnan.edu.cn. Tel: 0086-510-85912007. Fax: 0086-510-85912009.

Notes

The authors declare no competing financial interest.

ACKNOWLEDGMENTS

This research was financially supported by the National High-tech R&D Program of China (2012AA030313), Changjiang Scholars and Innovative Research Team in University (IRT1135), National Natural Science Foundation of China (51006046, 51203064, 21201083, and 51163014), the Priority Academic Program Development of Jiangsu Higher Education Institutions, Industry-Academia-Research Joint Innovation Fund of Jiangsu Province (BY2012068), Science and Technology Support Program of Jiangsu Province (SBE201201094), Industry-Academia-Research Prospective Joint Research Program of Jiangsu Province (SBY201220335), and the Innovation Program for Graduate Education in Jiangsu Province (CXZZ13_07).

REFERENCES

(1) Karim, F.; Fakhruddin, A. N. M. Recent Advances in the Development of Biosensor for Phenol: A Review. *Rev. Environ. Sci. Bio/Technol.* **2012**, *11*, 261−274.

(2) Zhou, X. H.; Liu, L. H.; Bai, X.; Shi, H. C. A Reduced Graphene Oxide Based Biosensor for High-Sensitive Detection of Phenols in Water Samples. *Sens. Actuators, B* **2013**, *181*, 661−667.

(3) Clement, R. E.; Eiceman, G. A.; Koester, C. J. Environmental-Analysis. *Anal. Chem.* **1995**, *67*, R221−R255.

(4) Barek, J.; Ebertova, H.; Mejstrik, V.; Zima, J. Determination of 2-Nitrophenol, 4-Nitrophenol, 2-Methoxy-5-Nitrophenol, and 2,4-Dinitrophenol by Differential-Pulse Voltammetry and Adsorptive Stripping Voltammetry. *Collect. Czech. Chem. Commun.* **1994**, *59*, 1761−1771.

(5) Ziętek, M. Über Die Polarographische Bestimmung von Parathion und Seinem Metabolit p-Nitrophenol in Blutextrakten. *Microchim. Acta* **1975**, 463−470.

(6) Solomon, E. I.; Lowery, M. D. Electronic-Structure Contributions to Function in Bioinorganic Chemistry. *Science* **1993**, *259*, 1575−1581.

(7) Li, Y.; Qin, C.; Chen, C.; Fu, Y.; Ma, M.; Xie, Q. Highly Sensitive Phenolic Biosensor Based on Magnetic Polydopamine-Laccase-Fe_3O_4 Bionanocomposite. *Sens. Actuators, B* **2012**, *168*, 46−53.

(8) Shimomura, T.; Itoh, T.; Sumiya, T.; Hanaoka, T.-a.; Mizukami, F.; Ono, M. Amperometric Detection of Phenolic Compounds with Enzyme Immobilized in Mesoporous Silica Prepared by Electrophoretic Deposition. *Sens. Actuators, B* **2011**, *153*, 361−368.

(9) Tan, Y.; Deng, W.; Ge, B.; Xie, Q.; Huang, J.; Yao, S. Biofuel Cell and Phenolic Biosensor Based on Acid-Resistant Laccase-Glutaraldehyde Functionalized Chitosan-Multiwalled Carbon Nanotubes Nanocomposite Film. *Biosens. Bioelectron.* **2009**, *24*, 2225−2231.

(10) Brondani, D.; de Souza, B.; Souza, B. S.; Neves, A.; Vieira, I. C. PEI-Coated Gold Nanoparticles Decorated with Laccase: A New Platform for Direct Electrochemistry of Enzymes and Biosensing Applications. *Biosens. Bioelectron.* **2013**, *42*, 242−247.

(11) Lee, S.; Ringstrand, B. S.; Stone, D. A.; Firestone, M. A. Electrochemical Activity of Glucose Oxidase on a Poly(Ionic Liquid)-

Au Nanoparticle Composite. *ACS Appl. Mater. Interfaces* **2012**, *4*, 2311−2317.
(12) Guo, C. X.; Sheng, Z. M.; Shen, Y. Q.; Dong, Z. L.; Li, C. M. Thin-Walled Graphitic Nanocages as a Unique Platform for Amperometric Glucose Biosensor. *ACS Appl. Mater. Interfaces* **2010**, *2*, 2481−2484.
(13) Saadati, S.; Salimi, A.; Hallaj, R.; Rostami, A. Layer by Layer Assembly of Catalase and Amine-Terminated Ionic Liquid onto Titanium Nitride Nanoparticles Modified Glassy Carbon Electrode: Study of Direct Voltammetry and Bioelectrocatalytic Activity. *Anal. Chim. Acta* **2012**, *753*, 32−41.
(14) Cai, C. J.; Xu, M. W.; Bao, S. J.; Lei, C.; Jia, D. Z. A Facile Route for Constructing a Graphene-Chitosan-ZrO_2 Composite for Direct Electron Transfer and Glucose Sensing. *RSC Adv.* **2012**, *2*, 8172−8178.
(15) Lee, J. H.; Park, J. Y.; Min, K.; Cha, H. J.; Choi, S. S.; Yoo, Y. J. A Novel Organophosphorus Hydrolase-Based Biosensor Using Mesoporous Carbons and Carbon Black for the Detection of Organophosphate Nerve Agents. *Biosens. Bioelectron.* **2010**, *25*, 1566−1570.
(16) Zheng, J.; Xu, J. L.; Jin, T. B. H.; Wang, J. L.; Zhang, W. Q.; Hu, Y. X.; He, P. G.; Fang, Y. Z. Preparation of Magnetic Ordered Mesoporous Carbon Composite and Its Application in Direct Electrochemistry of Horseradish Peroxidase. *Electroanalysis* **2013**, *25*, 2159−2165.
(17) Vamvakaki, V.; Tsagaraki, K.; Chaniotakis, N. Carbon Nanofiber-Based Glucose Biosensor. *Anal. Chem.* **2006**, *78*, 5538−5542.
(18) De Jong, K. P.; Geus, J. W. Carbon Nanofibers: Catalytic Synthesis and Applications. *Catal. Rev.* **2000**, *42*, 481−510.
(19) Zhao, X. F.; Qiu, J. S.; Sun, Y. X.; Hao, C.; Sun, T. J.; Cui, L. W. Fabrication of Carbon Nanofibres and Bamboo-Shaped Carbon Nanotubes with Open Ends from Anthracite Coal by Arc Discharge. *New Carbon Mater.* **2009**, *24*, 109−113.
(20) Guo, T.; Nikolaev, P.; Rinzler, A. G.; Tomanek, D.; Colbert, D. T.; Smalley, R. E. Self-Assembly of Tubular Fullerenes. *J. Phys. Chem.* **1995**, *99*, 10694−10697.
(21) Boskovic, B. O.; Stolojan, V.; Khan, R. U. A.; Haq, S.; Silva, S. R. P. Large-Area Synthesis of Carbon Nanofibres at Room Temperature. *Nat. Mater.* **2002**, *1*, 165−168.
(22) Wang, Y.; Serrano, S.; Santiago-Aviles, J. J. Raman Characterization of Carbon Nanofibers Prepared Using Electrospinning. *Synth. Met.* **2003**, *138*, 423−427.
(23) Liu, Y.; Hou, H. Q.; You, T. Y. Synthesis of Carbon Nanofibers for Mediatorless Sensitive Detection of NADH. *Electroanalysis* **2008**, *20*, 1708−1713.
(24) Huang, J.; Wang, D.; Hou, H.; You, T. Electrospun Palladium Nanoparticle-Loaded Carbon Nanofibers and Their Electrocatalytic Activities towards Hydrogen Peroxide and NADH. *Adv. Funct. Mater.* **2008**, *18*, 441−448.
(25) Tang, X.; Liu, Y.; Hou, H.; You, T. A Nonenzymatic Sensor for Xanthine Based on Electrospun Carbon Nanofibers Modified Electrode. *Talanta* **2011**, *83*, 1410−1414.
(26) Liu, Y.; Teng, H.; Hou, H.; You, T. Nonenzymatic Glucose Sensor Based on Renewable Electrospun Ni Nanoparticle-Loaded Carbon Nanofiber Paste Electrode. *Biosens. Bioelectron.* **2009**, *24*, 3329−3334.
(27) Wang, W.; Xu, Y.; Wang, D. I. C.; Li, Z. Recyclable Nanobiocatalyst for Enantioselective Sulfoxidation: Facile Fabrication and High Performance of Chloroperoxidase-Coated Magnetic Nanoparticles with Iron Oxide Core and Polymer Shell. *J. Am. Chem. Soc.* **2009**, *131*, 12892−12893.
(28) Lee, I. S.; Lee, N.; Park, J.; Kim, B. H.; Yi, Y.-W.; Kim, T.; Kim, T. K.; Lee, I. H.; Paik, S. R.; Hyeon, T. NiNiO CoreShell Nanoparticles for Selective Binding and Magnetic Separation of Histidine-Tagged Proteins. *J. Am. Chem. Soc.* **2006**, *128*, 10658−10659.
(29) Gao, J. H.; Gu, H. W.; Xu, B. Multifunctional Magnetic Nanoparticles: Design, Synthesis, and Biomedical Applications. *Acc. Chem. Res.* **2009**, *42*, 1097−1107.
(30) Willner, I.; Katz, E. Magnetic Control of Electrocatalytic and Bioelectrocatalytic Processes. *Angew. Chem., Int. Ed.* **2003**, *42*, 4576−4588.
(31) Yang, Z. P.; Zhang, C. J.; Zhang, J. X.; Bai, W. B. Potentiometric Glucose Biosensor Based on Core-Shell Fe_3O_4-Enzyme-Polypyrrole Nanoparticles. *Biosens. Bioelectron.* **2014**, *51*, 268−273.
(32) Peng, H. P.; Liang, R. P.; Zhang, L.; Qiu, J. D. General Preparation of Novel Core-Shell Heme Protein-Au-Polydopamine-Fe_3O_4 Magnetic Bionanoparticles for Direct Electrochemistry. *J. Electroanal. Chem.* **2013**, *700*, 70−76.
(33) Clarke, S. J.; Hollmann, C. A.; Zhang, Z.; Suffern, D.; Bradforth, S. E.; Dimitrijevic, N. M.; Minarik, W. G.; Nadeau, J. L. Photophysics of Dopamine-Modified Quantum Dots and Effects on Biological Systems. *Nat. Mater.* **2006**, *5*, 409−417.
(34) Liu, A. H.; Wei, M. D.; Honma, I.; Zhou, H. S. Biosensing Properties of Titanate-Nanotube Films: Selective Detection of Dopamine in the Presence of Ascorbate and Uric Acid. *Adv. Funct. Mater.* **2006**, *16*, 371−376.
(35) Njagi, J.; Chernov, M. M.; Leiter, J. C.; Andreescu, S. Amperometric Detection of Dopamine in Vivo with an Enzyme Based Carbon Fiber Microbiosensor. *Anal. Chem.* **2010**, *82*, 989−996.
(36) Fu, Y.; Li, P.; Xie, Q.; Xu, X.; Lei, L.; Chen, C.; Zou, C.; Deng, W.; Yao, S. One-Pot Preparation of Polymer-Enzyme-Metallic Nanoparticle Composite Films for High-Performance Biosensing of Glucose and Galactose. *Adv. Funct. Mater.* **2009**, *19*, 1784−1791.
(37) An, P.; Zuo, F.; Wu, Y. P.; Zhang, J. H.; Zheng, Z. H.; Ding, X. B.; Peng, Y. X. Fast Synthesis of Dopamine-Coated Fe_3O_4 Nanoparticles through Ligand-Exchange Method. *Chin. Chem. Lett.* **2012**, *23*, 1099−1102.
(38) Mazur, M.; Krywko-Cendrowska, A.; Krysinski, P.; Rogalski, J. Encapsulation of Laccase in a Conducting Polymer Matrix: A Simple Route towards Polypyrrole Microcontainers. *Synth. Met.* **2009**, *159*, 1731−1738.
(39) Wang, K.; Tang, J.; Zhang, Z.; Gao, Y.; Chen, G. Laccase on Black Pearl 2000 Modified Glassy Carbon Electrode: Characterization of Direct Electron Transfer and Biological Sensing Properties for Pyrocatechol. *Electrochim. Acta* **2012**, *70*, 112−117.
(40) Laviron, E. General Expression of the Linear Potential Sweep Voltammogram in the Case of Diffusionless Electrochemical Systems. *J. Electroanal. Chem. Interfacial Electrochem.* **1979**, *101*, 19−28.
(41) Zhou, X. H.; Huang, X. R.; Liu, L. H.; Bai, X.; Shi, H. C. Direct Electron Transfer Reaction of Laccase on a Glassy Carbon Electrode Modified with 1-Aminopyrene Functionalized Reduced Graphene Oxide. *RSC Adv.* **2013**, *3*, 18036−18043.
(42) Rahman, M. A.; Noh, H. B.; Shim, Y. B. Direct Electrochemistry of Laccase Immobilized on Au Nanoparticles Encapsulated-Dendrimer Bonded Conducting Polymer: Application for a Catechin Sensor. *Anal. Chem.* **2008**, *80*, 8020−8027.
(43) Liu, Y.; Qu, X.; Guo, H.; Chen, H.; Liu, B.; Dong, S. Facile Preparation of Amperometric Laccase Biosensor with Multifunction Based on the Matrix of Carbon Nanotubes−Chitosan Composite. *Biosens. Bioelectron.* **2006**, *21*, 2195−2201.
(44) Xu, X.; Lu, P.; Zhou, Y.; Zhao, Z.; Guo, M. Laccase Immobilized on Methylene Blue Modified Mesoporous Silica MCM-41/PVA. *Mater. Sci. Eng., C* **2009**, *29*, 2160−2164.
(45) Xu, X.; Guo, M.; Lu, P.; Wang, R. Development of Amperometric Laccase Biosensor through Immobilizing Enzyme in Copper-Containing Ordered Mesoporous Carbon (Cu-OMC)/Chitosan Matrix. *Mater. Sci. Eng., C* **2010**, *30*, 722−729.